Journal of Photochemistry and Photobiology A: Chemistry 231 (2012) 64–69

Contents lists available at SciVerse ScienceDirect

Journal of Photochemistry and Photobiology A: Chemistry

journal homepage: www.elsevier.com/locate/jphotochem

Iodine-free solid-state dye-sensitized solar cells with fullerene derivatives as hole transporting materials

Ki-Suck Jung[a,b], Su-Bin Lee[a], Young-Keun Kim[a,c], Min-Hye Seo[a], Won-Pill Hwang[a], Young-Wook Jang[a,c], Hyun-Woo Park[a,c], Bo-Ra Jin[d], Mi-Ra Kim[a,*], Jin-Kook Lee[a,**]

[a] Department of Polymer Science & Engineering, Pusan National University, Jangjeon-dong, Kuemjeong-gu, Busan 609-735, South Korea
[b] Daehan Solvay Special Chemical Co., Ltd., Daejing-ri, Onsan-eup, Ulju-kun, Ulsan 689-892, South Korea
[c] Solchem Co., Ltd., Jangjeon-dong, Kuemjeong-gu, Busan 609-735, South Korea
[d] Department of Chemistry, Pusan National University, Jangjeon-dong, Kuemjeong-gu, Busan 609-735, South Korea

ARTICLE INFO

Article history:
Received 28 March 2011
Received in revised form
21 November 2011
Accepted 7 January 2012
Available online 14 January 2012

Keywords:
DSSC
Fullerene derivatives
Hole transporting materials

ABSTRACT

This study focuses on the syntheses of N,N-dimethyl-2-thiophenyl-3,4-fulleropyrrolidium iodide (DMFPI), poly N-methyl-2-thiophenyl-3,4-fulleropyrrolidine-co-3-hexylthiophene (MFP-co-3HT), poly N-methyl-2-thiophenyl-3,4-fulleropyrrolidine-co-3-dodecylthiophene (MFP-co-3DT), and poly N-methyl-2-thiophenyl-3,4-fulleropyrrolidine-co-3-thiopheneacetic acid (MFP-co-3TA) and their photovoltaic properties as hole transporting materials (HTMs) for use in DSSCs. The synthesized DMFPI and copolymers were characterized by ^{1}H NMR, MALDI TOF-mass spectrometry, UV–vis spectroscopy, and cyclic voltammetry. The DSSC devices were fabricated and their photovoltaic performances were measured using a solar simulator under AM 1.5 illumination.

1. Introduction

Dye-sensitized solar cells (DSSCs) are one of the promising candidates for the next generation of solar cells, because of their simple structure with a relatively high conversion efficiency and inexpensive fabrication procedures compared to solar cells based on amorphous silicon, DSSCs based on liquid electrolytes have reached efficiencies as high as 10% under AM 1.5 [1–4], but the use of liquid electrolytes has created a lot of difficulties in terms of the sealing and long-term photochemical stability of the devices [5–7]. An effective approach to solve this problem is the replacement of the volatile liquid electrolyte with a solid-state or quasi-solid state hole conductor, such as a p-type semiconductor [8,9], ionic liquid electrolyte [10] and polymer electrolyte [11,12].

Among these hole conductors, p-type semiconductors constitute the most common approach to fabricate solid-state DSSCs. There are several requirements for a p-type semiconductor to be used in a DSSC. However, the familiar large-band gap inorganic p-type semiconductors such as SiC and GaN are not suitable for use in DSSCs [13], because they can degrade the dye during the high-temperature deposition techniques. On the other hand, CuI is suitable for use in a DSSC, because of its suitable bandgap and deposition. Tennakone et al. [14] reported an efficiency of 2.4% in solid-state DSSCs made with CuI. Compared with inorganic p-type semiconductors, organic p-type semiconductors possess the advantages of having plentiful sources, easy film formation and low cost [15–17]. Recently, the efficiency of cells using poly(3,4-ethylenedioxythiophene) as the hole conductor was reported to be 2.85% [18]. The cells were fabricated without iodine (I_2) and the highest efficiency was obtained using PEDOT as the hole transporting material (HTM). Fullerene [C_{60}] is a molecule with remarkable charge transfer properties, which has been used for the preparation of a wide variety of different electroactive systems [19]. According to theoretical calculations, it exhibits a triply degenerated LUMO comparatively low in energy. Saito and Oshiyama [20] using a one-electron model calculated the HOMO–LUMO gap to be 1.92 eV for the free C_{60} molecule and the direct band gap to be 1.5 eV for the crystal. The latter value is close to the experimental value of ~1.6 eV for the fundamental edge in the optical absorption spectra [21] and photoconductivity spectra [22] of C_{60} thin films.

Therefore, C_{60} behaves as an electronegative molecule which reversibly accepts up to six electrons in solution [23–25]. The cyclic voltammetry and electron affinity measured for C_{60} clearly confirm that it is a moderate electron acceptor comparable to other organic molecules such as benzo- and naphtho-quinones [26,27]. This electron-accepting ability of C_{60} to form stable multi-anions [28,29] is in sharp contrast to its ability to generate very

* Corresponding author. Tel.: +82 51 510 3045.
** Corresponding author.
E-mail addresses: mrkim2@pusan.ac.kr (M.-R. Kim), leejk@pusan.ac.kr (J.-K. Lee).

1010-6030/$ – see front matter © 2012 Elsevier B.V. All rights reserved.
doi:10.1016/j.jphotochem.2012.01.005

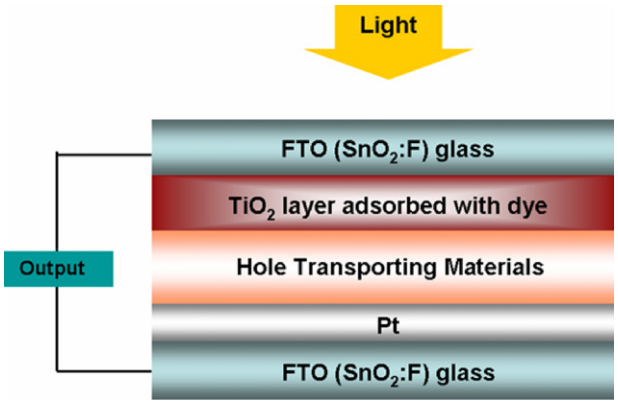

Fig. 1. The structure of DSSC device with hole transporting materials.

unstable cationic species [30–33]. Therefore, we synthesized an HTM based on soluble fullerene derivatives for use with free-iodine (I_2), viz. N,N-dimethyl-2-thiophenyl-3,4-fulleropyrrolidium iodide (DMFPI), and studied its application to DSSCs and also synthesized thiophene group substituted fulleropyrrolidine derivatives for use as polymer HTMs.

We prepared DSSC devices, sandwiched with TiO_2 adsorbed dyes and Pt-coated electrode as the two electrodes. The photovoltaic effect of the FTO/TiO_2/Dye/HTML (hole transporting materials layer)/Pt device (Fig. 1) was measured by a solar simulator under AM 1.5 conditions. The power conversion efficiency (η) of the solar cell device was calculated from the values of the open-circuit voltage (V_{oc}) and short-circuit current (J_{sc}), and the fill factor (FF) was calculated from the values of V_{oc}, J_{sc}, and η.

2. Experimental

2.1. Materials

Fullerene [C_{60}] (98%), 3-thiophene-carboxaldehyde (98%), sarcosine (98%), iodomethane (CH_3I, 99%), 3-hexylthiophene (3HT), 3-dodecylthiophene (3DT), 3-thiopheneacetic acid (3TA) and

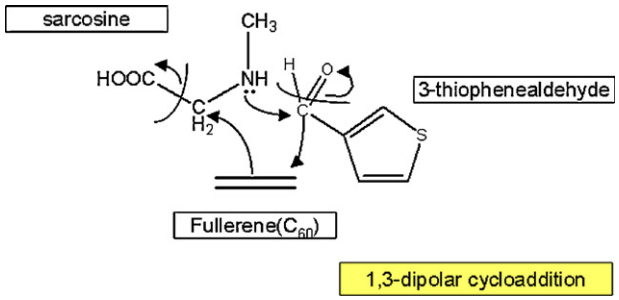

Fig. 2. 1,3-Dipolar cycloadditon.

anhydrous iron(III) chloride were purchased from Aldrich Co. and used without further purification. All other chemicals were of reagent grade and used without further purification.

Ruthenium dyes such as *cis*-bis(isothiocyanato)bis(2,2′-bipyridyl-4,4′-dicarboxylato)-ruthenium(II) dye (N3 dye), fluorine-doped SnO_2 glass (FTO glass, 15 Ω/square), 1-propyl-3-methylimidazolium iodide (PMII), TiO_2 pastes Ti-Nanoxide HT/SP (particle size: 9 nm) and Ti-Nanoxide R/SP (particle size: 300 nm), and Pt paste (Pt catalyst T/SP) were purchased from Solaronix. Acetic acid, triton X-100, acetylacetone, deionized water, iodine (I_2), propylene carbonate (PC), ethylene carbonate (EC), acetonitrile (AN), and tetrabutylammonium iodide (TBAI) were purchased from Aldrich Co. and used without further purification.

2.2. Measurements

In order to confirm the chemical structures, the ^{1}H NMR spectra were recorded using a Varian Unity Plus 300 (300 MHz) spectrophotometer using tetramethylsilane (TMS) as an internal standard. The UV–vis spectra were recorded using an Optizen 2120UV spectrophotometer and UVIKON 860 spectrophotometer. The electrochemical properties were measured by a Bioanalytical Systems CV-50 W voltammetric analyzer. The molecular weights were measured using micromass MALDI, matrix-assisted laser desorption ionization-time of flight-MS (MALDI-TOF-MS). To confirm

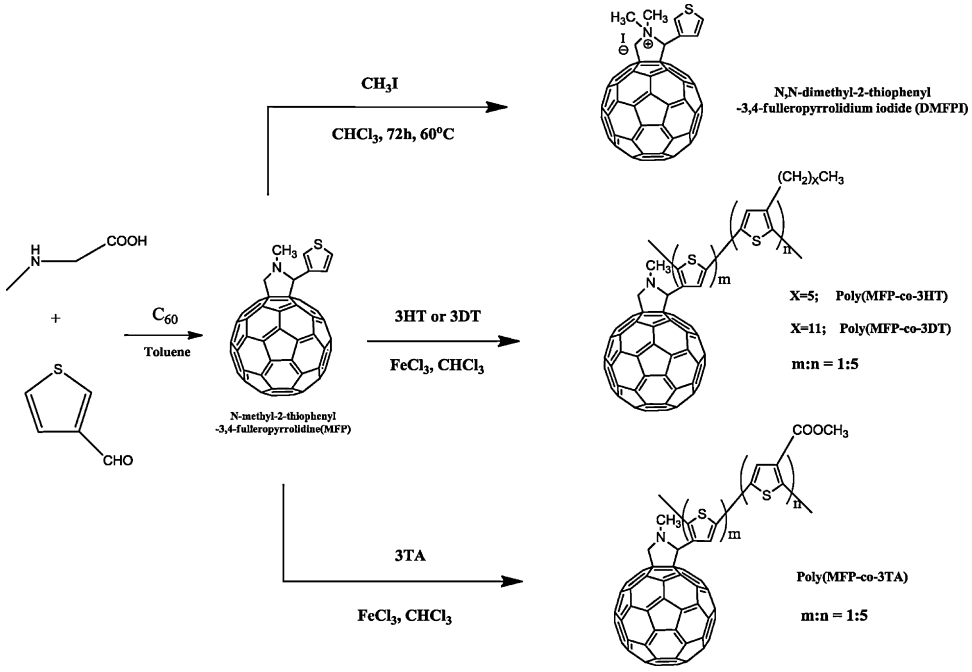

Fig. 3. The synthetic routes and chemical structures of MFP, DMFPI and copolymers.

Table 1
Solubility of C_{60}, MFP, DMFPI and copolymers.

Solvents	C_{60}	MFP	DMFPI	Poly(MFP-co-3HT)	Poly(MFP-co-3DT)	Poly(MFP-co-3TA)
Chloroform	I	S	I	S	S	S
Chlorobenzene	I[a]	S	I[a]	S	S	S
Toluene	I[a]	S	I	S	S	S
Acetone	I	I	I	I	I	I
Methanol	I	I	I	I	I	I
THF	I	S	S	S	S	S
NMP	I	S	S	S	S	S
DMF	I	I[a]	S	I[a]	I[a]	I[a]

Solubility in 100 mg/ml, S = soluble, I = insoluble.
[a] When it is heated to 100 °C, it is partially soluble.

the molecular weights of the copolymers, we used gel permeation chromatography (GPC) with polystyrene as a standard on a Waters (150GPC) at 40 °C in tetrahydrofuran (THF). The photovoltaic characteristics of the DSSC devices were measured using a Solar Simulator (150 W simulator, PEC-L11, PECCELL) under simulated solar light with an ARC Lamp power supply (AM 1.5, 100 mW/cm^2) with a black mask. The charge transfer resistances of the DSSCs were measured by the alternating current (AC) impedance test using an electrochemical impedance analyzer (Reference 600, GAMRY instruments). The blocking cell consisting of Pt/electrolyte solution/Pt was used in the frequency range of 1–10^6 Hz at room temperature. The applied bias voltage and ac amplitude were set to the open circuit voltage of the cells and 50 mV, respectively. The Electrochemical Impedance Spectroscopy (EIS) data were also measured with an impedance analyzer under the same conditions using FTO/TiO_2/electrolyte/Pt/FTO cells and fitted by Z-MAN software (WONATECH) and Echem analyst (GAMRY).

2.3. Synthesis of hole transporting materials (HTM)

2.3.1. Synthesis of fulleropyrrolidine salt hybrid

To synthesize the fullerene derivatives, we used the 1,3-dipolar cycloaddition of fullerene (Fig. 2) [34,35]. N-methyl-2-thiophenyl-3,4-fulleropyrrolidine (MFP) and DMFPI were synthesized using the synthetic route shown in Fig. 3, along with the chemical structure. A mixture of 112 mg of 3-thiophene-carboxaldehyde (1.00 mmol), 360 mg of fullerene [C_{60}] (0.50 mmol), and 89 mg of sarcosine (1.00 mmol) in 100 ml of toluene was heated at reflux temperature for 24 h. Chromatography on a silica column was used with toluene as the eluent and we obtained MFP in 21% yield. ^{1}H NMR (300 MHz, $CDCl_3$): δ 7.63–7.20 (m, thiophene), 5.08 (s, —N—CH—thiophene), 4.99 (d, —N—CH—thiophene), 4.23 (d, —N—CH_2—), 2.84 (m, N—CH_3), M/e = 859.

Then we synthesized DMFPI, a mixture of 100 mg of MFP (0.1164 mmol) and 12 ml of CH_3I in 24 ml of chloroform was refluxed with stirring for 3 days at 65 °C under argon. The MFP was reacted with CH_3I through N-alkylation and the product was obtained which was washed with toluene and hexane several times [34,36]. The solvent was removed under vacuum and the final product obtained in 75% yield. ^{1}H NMR (300 MHz, $CDCl_3$): δ 8.41–7.71 (m, thiophene), 7.40 (s, —N+—CH—thiophene), 6.04 (d, —N—CH_2—), 5.78 (d, —N—CH_2—), 4.19 (m, N+—CH_3), M/e = 873.

2.3.2. Synthesis of fulleropyrrolidine thiophene copolymers

The synthetic routes and chemical structures of the copolymers are shown in Fig. 3. A mixture of 100 mg of MFP (0.1164 mmol), 97 mg of 3HT (0.582 mmol), and 452 mg of anhydrous $FeCl_3$ in 40 ml of chloroform was stirred at room temperature for 6 h. The reaction mixture was then poured into a large quantity of methanol. The product was dissolved in toluene, chloroform, and then evaporated. The dark brown precipitate of poly N-methyl-2-thiophenyl-3,4-fulleropyrrolidine-co-3-hexylthiophene (MFP-co-3HT) was collected, and poly N-methyl-2-thiophenyl-3,4-fulleropyrrolidine-co-3-dodecylthiophene (MFP-co-3DT) and poly N-methyl-2-thiophenyl-3,4-fulleropyrrolidine-co-3-thiopheneacetic acid (MFP-co-3TA) were obtained using similar procedures and with the same molar ratios. **Poly(MFP-co-3HT)**: ^{1}H NMR (300 MHz, $CDCl_3$): δ 7.63–7.35 (m, thiophene), 7.00 (s, thiophene(3HT)), 4.82 (d, —N—CH—thiophene), 4.2 (d, —N—CH_2—), 2.84 (m, N-CH_3), 2.24–1.3 (m, —$(CH_2)_5$—CH_3). **Poly(MFP-co-3DT)**: ^{1}H NMR (300 MHz, $CDCl_3$): δ 7.62–7.36 (m, thiophene), 6.99 (s, thiophene (3DT)), 4.85 (d, —N—CH—thiophene), 4.2 (d, —N—CH_2—), 2.84 (m, N—CH_3), 2.20–0.8 (m, —$(CH_2)_{11}$—CH_3). **Poly(MFP-co-3TA)**: ^{1}H NMR (300 MHz, $CDCl_3$): δ 7.62–7.38 (m, thiophene), 7.15–7.10 (m, thiophene (3DT)), 4.98 (m, —N—CH—thiophene), 4.22 (d, —N—CH_2—), 2.80 (m, N—CH_3), 3.80–3.40 (m, —CH_2—$COOCH_3$).

2.4. Fabrication of dye-sensitized solar cell device

We prepared sandwich type DSSC devices composed of a nanocrystalline oxide film, Ruthenium complex dye, organic electrolyte, and Pt counter electrode. Two kinds of nanoparticle sized TiO_2 pastes were used (9 nm and 300 nm) for double layers. The 9 nm nanoparticle sized TiO_2 paste was used to adsorb the light, while the 300 nm nanoparticle sized TiO_2 paste was used as a light scattering layer. The nanocrystalline oxide film was prepared that TiO_2 pastes were spread evenly on an FTO glass using the doctor blade method and then sintered at 500 °C and its thickness was 12 μm. We used N3 dye as the Ruthenium complex dye to sensitize the light. The sensitizer, N3 dye, was dissolved in 20 ml of ethanol solution at a concentration of 7.5 mg for each device. The nanoporous TiO_2 film was immersed in the dye solution at 55 °C for at least 16 h to impregnate it with the dye. We prepared two kinds of electrolytes; the first electrolyte solution consisted of DMFPI and ethylene carbonate (EC)/propylene carbonate (PC) [EC/PC = 4:1 (v/v), 1 ml]. It was deposited onto the TiO_2 electrode adsorbed dyes and dried at about 55 °C for several hours to evaporate the solvent. The second electrolyte consisted of I_2 (12 mg), tetra butyl ammonium iodide (36 mg), and 1-propyl-3-methylimidazolium iodide (4 mg) in a solution of EC/PC/AN (acetonitrile) (4:1:5 v/v/v, 1 ml) and 20 mg of the copolymers in 1.5 ml of chloroform solution. The Pt pastes were also spread on an FTO glass using the doctor blade method and the Pt spread FTO glass was sintered at 450 °C. In assembling the DSSC devices, the working and counter electrodes were clamped together.

3. Results and discussion

3.1. Characterization of MFP, DMFPI, and copolymers

The chemical structures of MFP, DMFPI and the copolymers were characterized by ^{1}H NMR and their soluble properties were

Table 2
Molecular weight data of copolymers.

	M_n	M_w	PDI
Poly(MFP-co-3HT)	2100	6600	3.14
Poly(MFP-co-3DT)	11,200	20,700	1.85
Poly(MFP-co-3TA)	5400	12,200	2.26

appeared in Table 1. The measurements showed that DMFPI was downfield shifted compared to MFP due to its ionization, because it was less shielded. In particular, the methyl group attached to nitrogen was downfield shifted. The alkyl chain peaks of poly(MFP-co-3HT) and poly(MFP-co-3DT) were observed at 0.8–2.24 ppm and that of the methoxy group of poly(MFP-co-3TA) was observed at around 3.5 ppm.

Using MALDI-TOF MASS spectroscopy, we estimated the molecular weights of MFP and DMFPI. The molecular weights of the copolymers were estimated by gel permeation chromatography (GPC) in THF (Table 2). The molecular weight is very important due to the interpenetration of the electrolytes. We tuned the weight average molecular weight (M_w) of the copolymer to 7000–20,000 g/mol, which is known to be suitable. We obtained copolymers having M_w values of 6700 g/mol (poly(MFP-co-3HT)), 20,700 g/mol (poly(MFP-co-3DT)), and 12,200 g/mol (poly(MFP-co-3TA)).

3.2. Optical properties of MFP, DMFPI, and copolymers

In order to use the copolymers as HTMs in DSSCs, they should not absorb light in the visible spectrum. We measured the UV–vis absorption spectra of DMFPI in chlorobenzene solution. This solution was prepared by adding 0.2 mg of C_{60} or fullerene derivatives to 4 ml of pure chlorobenzene solution. Fig. 4 shows that the maximum absorption peak of DMFPI in chlorobenzene solution appeared at 345 nm and the maximum absorption peaks of MFP and the copolymers in chloroform solution appeared at 329 nm and 308 nm, respectively, corresponding to the fulleropyrrolidine group. The absorbance spectra of the copolymers broadly appeared in the range of 300–550 nm after the formation of the copolymer. They absorbed very little light in the visible spectrum and were therefore suitable for use as HTMs.

3.3. Cyclic voltammetry

Cyclic voltammetry (CV) was used for measuring the electrochemical transfer and estimating the HOMO and LUMO energy levels [37]. We used CV to confirm the band energy of DMFPI and the copolymers. The redox data were standardized with the ferrocene–ferricenium couple, which has a calculated energy of −4.8 eV [37]. The reference electrode was Ag/Ag^+ and the working and counter electrodes were Pt wires. The energy bandgap was calculated from Eqs. (1) and (2) [38],

$$E_g = h\nu_{1\,or\,2}\ \ (\mathrm{J}) = \frac{1240}{\lambda_{1\,or\,2}}\ \ (\mathrm{eV}) \tag{1}$$

$$\mathrm{LUMO} = \mathrm{HOMO} - E_g \tag{2}$$

where h is the Planck constant, ν is the frequency, and λ is the wavelength of the absorption (λ_1) or the fluorescence (λ_2) edge.

In order for them to be used as a HTMs, the upper edge level of the valence band of DMFPI and the copolymers must be higher than the ground state level of the dye. In other words, the HTML should accept the holes from the dye cations [39]. That is,

$$S + h\nu \rightarrow S^*$$

$$S^* \rightarrow S^+ + e^- \quad (\text{to conduction band of } TiO_2)$$

$$S^+ \rightarrow S + h^+ \quad (\text{to valence band of HTM})$$

The HOMO level of DMFPI of 4.97 eV was higher than the ground state level of the dye, viz. 5.7 eV (Table 3). We confirmed that DMFPI was a suitable hole conductor with an appropriate band gap. The HOMO levels of poly(MFP-co-3HT), poly(MFP-co-3TA) of 5.50 eV and 5.55 eV, respectively, were higher than the redox potential of the iodine redox couple and lower than the work function of the Pt counter electrode. It was found that they have proper levels for the transfer of the hole charges between the oxidized dyes and polymer redox electrolyte. Due to the good charge transfer ability of poly(MFP-co-3HT) and poly(MFP-co-3TA), the J_{sc} values of the corresponding DSSC devices were increased and this led to an improvement in their efficiency. When using poly(MFP-co-3DT), however, the HOMO level of poly(MFP-co-3DT) was similar to the energy level of the oxidized dyes, with the result that is hard to transfer the hole charges. As a result of the inappropriate energy level the efficiency of the DSSC device with poly(MFP-co-3DT) was decreased compared to those of the other devices. The energy band diagram of the hole transfer mechanism is illustrated in Fig. 5.

3.4. Photovoltaic performances of FTO/TiO_2/Dye/HTML/Pt devices

The photovoltaic performances of the DSSC devices were studied by measuring their photocurrent density–voltage (I–V) characteristics under light illumination. The power conversion efficiency (η) of the devices is given by Eq. (3)

$$\eta = \frac{P_{max}}{P_{in}} = \frac{(J_{sc} \times V_{oc}) \times FF}{P_{in}} \quad \text{with} \quad FF = \frac{P_{max}}{J_{sc} \times V_{oc}} = \frac{J_{max} \times V_{max}}{J_{sc} \times V_{oc}} \tag{3}$$

where P_{max} is the output electrical power of the device under illumination, and P_{in} represents the intensity of the incident light (e.g., in W/m^2 or mW/cm^2). V_{oc} is the open-circuit voltage, J_{sc} is the short-circuit current density, and the fill factor (FF) is calculated from the values of V_{oc}, J_{sc}, and the maximum power point, P_{max}.

We measured the I–V curves of the FTO/TiO_2/Dye/HTML/Pt devices using DMFPI or the copolymers as the HTM. The photovoltaic performances of the DSSC devices are summarized in Table 4. In order to use DMFPI as the HTM, several conditions need to be satisfied. Firstly, the HOMO of the dye should be located under the HOMO of the HTM, in order to smooth the charge transfer of the holes from the dye. This is essential for the charge transfer between the dyes and TiO_2 (electron) or dyes and HTM (holes). It is important

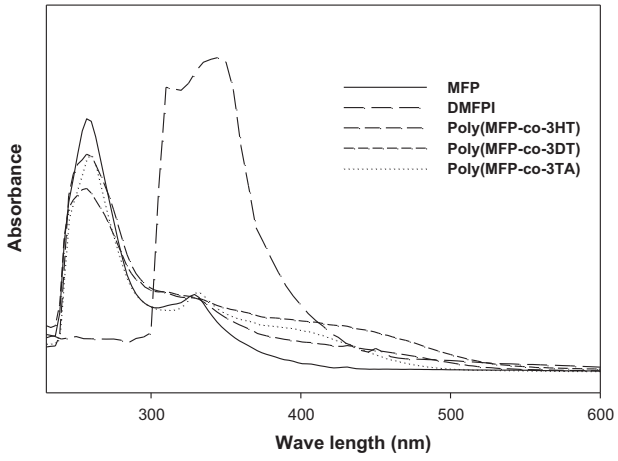

Fig. 4. UV–vis spectra of MFP, copolymers (chloroform) and DMFPI (chlorobenzene).

Table 3
Cyclic voltammetry (CV) data of DMFPI and copolymers.

Compounds	$E^{+1}_{1/2}$ (V)	Optical bandgap in film (eV)	HOMO[b]	LUMO[b]
DMFPI[a]	0.24	2.80[d]	4.97[c]	2.17[c]
Poly(MFP-co-3HT)[a]	0.95	2.32[d]	5.50[c]	3.18[c]
Poly(MFP-co-3DT)[a]	0.99	2.39[d]	5.61[c]	3.22[c]
Poly(MFP-co-3TA)[a]	0.92	2.37[d]	5.55[c]	3.18[c]

[a] DMFPI vs Fc/Fc+ were determined in solution state with 0.1 M TBAP (tetra butyl ammonium perchlorate) in dimethyl sulfoxide (DMSO) and copolymers vs Fc/Fc+ were determined in solution state with 0.1 M TBAP (tetra butyl ammonium hexafluorophosphate) in dichloromethane (CH_2Cl_2).
[b] Set ferrocene–ferrocenium = 4.8 eV.
[c] From $E^{-1}_{1/2}$ (V) and bandgap in film.
[d] From onset potential and optical bandgap in film.

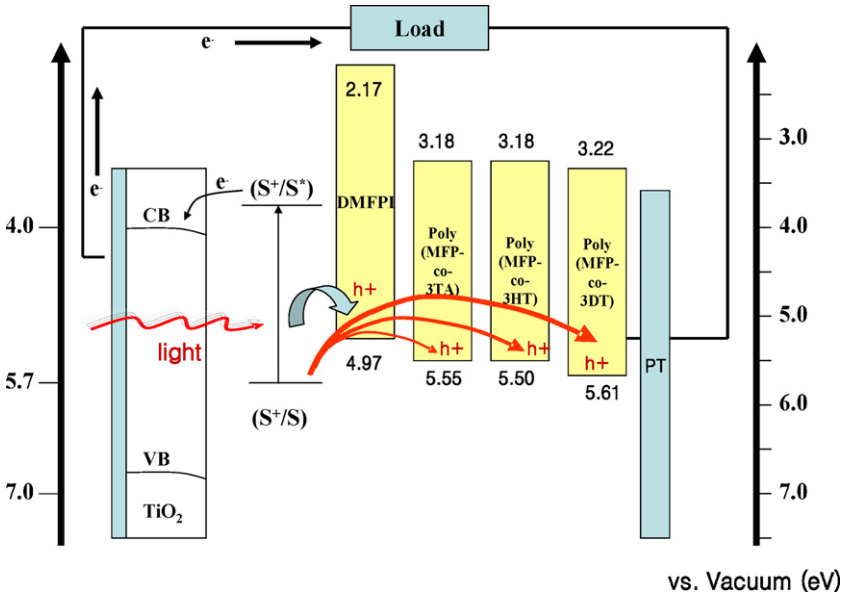

Fig. 5. The energy band diagram of the charge transfer mechanism with HTM (hole transporting materials).

Table 4
The photocurrent–voltage characteristics of the DSSC devices with hole transporting materials (DMFPI) under AM 1.5, active area: 0.25 cm^2.

Electrolytes	V_{oc} (V)	J_{sc} (mA/cm^2)	Fill factor	Efficiency (%)
EC + PC (4:1 (v/v))	0.17	0.06	0.190	0.0019
EC + PC (4:1 (v/v)) + DMFPI	0.53	10.5	0.414	2.31

to balance the energy level of the dyes and the HTM. Secondly, the HTM should not absorb light in visible region. Thirdly, it is the suitability with the dyes. In our study, we attempted to maintain the material using DMF as the solvent, however it was not appropriate for the dyes because the DMF dissolved the dyes and also degraded the dyes on the TiO_2 nanocrystallites. We chose ethylene carbonate (EC) and propylene carbonate (PC), which have good ionic conductivity [40,41], as the solvent, since these materials have already been used in quasi-solid-state DSSCs. The solvent is helpful to dissociate the iodide salts and therefore facilitate the transfer of the charges. We measured the cell performance and obtained a J_{sc} of 10.5 mA/cm^2, a V_{oc} of 0.530 V and FF of 0.414. The efficiency of the device was 2.31%, which is remarkable when using an HTM without additives (see Table 5).

In the devices using poly(MFP-co-3HT), poly(MFP-co-3DT) and poly(MFP-co-3TA) with iodine, the J_{sc} values are 4.4, 4.4 and 7.6 mA/cm^2, the V_{oc} values are 0.615, 0.583 and 0.621 V and the FF values are 0.532, 0.541 and 0.586, leading to calculated η values of 1.45, 1.38 and 2.75%, respectively. Poly(MFP-co-3TA) showed the best efficiency, because of its appropriate hole transfer level. We

Table 5
The photocurrent–voltage characteristics of the DSSC devices under AM 1.5, active area: 0.36 cm^2.

	V_{oc} (V)	J_{sc} (mA/cm^2)	Fill factor	Efficiency (%)
Poly(MFP-co-3HT)[a]	0.615	4.4	0.532	1.45
Poly(MFP-co-3HT)[b]	0.714	2.3	0.666	1.09
Poly(MFP-co-3DT)[a]	0.583	4.4	0.541	1.38
Poly(MFP-co-3DT)[b]	0.690	1.9	0.599	0.79
Poly(MFP-co-3TA)[a]	0.621	7.6	0.586	2.75
Poly(MFP-co-3TA)[b]	0.724	4.5	0.615	1.98

[a] The DSSC devices using polymer electrolyte with iodine (I_2).
[b] The DSSC devices using polymer electrolyte without iodine (I_2).

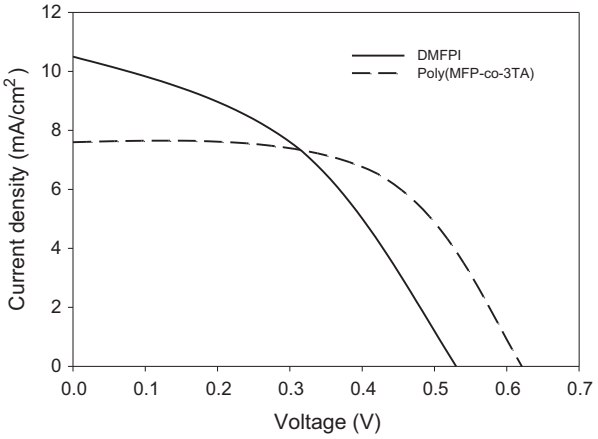

Fig. 6. *I–V* curve of DSSCs using DMFPI without iodine (I_2) under AM 1.5, active area: 0.25 cm^2 and using poly(MFP-co-3TA) with iodine (I_2) under AM 1.5, active area: 0.36 cm^2.

investigated the DSSC devices without iodine (I_2). The disadvantage of the DSSCs using I_2 is their poor long-term stability, due to sublimation. I_2 is colored and absorbs solar light in the visible region. To overcome this drawback, we attempted to fabricate DSSC devices without any iodine in the electrolyte. The cell without I_2 showed a lower efficiency than the DSSCs using I_2. In the DSSC performance, V_{oc} dramatically increased, but J_{sc} decreased compared to the DSSC using I_2. The efficiencies of the devices using the copolymer electrolytes without iodine, poly(MFP-co-3HT), poly(MFP-co-3DT) and poly(MFP-co-3TA) were as follows: J_{sc} values of 2.3, 1.9 and 4.5 mA/cm^2, V_{oc} values of 0.714, 0.690 and 0.724 V, FF values of 0.666, 0.599 and 0.615 and η values of 1.09, 0.79 and 1.98%, respectively. And the *I–V* curve for DSSC device that gives an efficiency above 2% in Fig. 6.

4. Conclusion

We focused on the fabrication and investigation of the photovoltaic properties of DSSC devices based on soluble fullerene derivatives.

In this work, we successfully synthesized the organic HTM, DMFPI, and fabricated DSSC devices [FTO/TiO_2/dye/HTML/Pt] using this material as the HTM. The best result of the DSSC devices was a power conversion efficiency of 2.31% using DMFPI without any additives. We confirmed the hole transfer mechanism and the effect of the HTML on the performance of the DSSC device.

In addition, we successfully fabricated DSSC devices using fullerene copolymers. It was found that the DSSC devices using poly(MFP-co-3HT), poly(MFP-co-3DT), and poly(MFP-co-3TA) as the HTM showed efficiencies of 1.45%, 1.38% and 2.75% respectively. When using poly(MFP-co-3HT), poly(MFP-co-3DT), and poly(MFP-co-3TA) as the HTM without iodine (I_2), we obtained efficiencies of 1.09%, 0.79%, 1.98%, respectively.

Acknowledgements

This research was supported by the Converging Research Center Program through the National Research Foundation of Korea (NRF) funded by the Ministry of Education, Science and Technology (20090082141).

References

[1] A. Hagffeldt, M. Grätzel, Chem. Rev. 95 (1995) 49–68.
[2] A. Goetzberger, J. Luther, G. Willeke, Sol. Energy Mater. Sol. Cells 74 (1–4) (2002) 1–11.
[3] M.A. Green, Solar Energy 76 (1–3) (2004) 3–8.
[4] M.K. Nazeeruddin, A. Kay, I. Rodicio, R. Humphry-Baker, E. Mueller, P. Liska, N. Vlachopoulos, M. Graetzel, J. Am. Chem. Soc. 115 (14) (1993) 6382–6390.
[5] N. Papageorgiou, W.F. Maier, M. Grätzel, J. Electrochem. Soc. 144 (3) (1997) 876–884.
[6] A. Kay, M. Gratzel, Sol. Energy Mater. Sol. Cells 44 (1996) 99–117.
[7] J.R. Durrant, S.A. Haque, Nat. Mater. 2 (2003) 362–363.
[8] K. Tennakone, G.R.R.A. Kumara, I.R.M. Kottegoda, K.G.U. Wijayantha, V.P.S. Perera, J. Phys. D: Appl. Phys. 31 (1998) 1492–1496.
[9] B. O'Regan, D.T. Schwartz, S. Zakeeruddin, Mohammed, M. Gratzel, Adv. Mater. 12 (17) (2000) 1263–1267.
[10] N. Papageorgiou, Y. Athanassov, M. Armand, P. Bonhote, H. Pettersson, A. Azam, M. Graetzel, J. Electrochem. Soc. 143 (10) (1996) 3099–3108.
[11] A.F. Nogueira, De P. Marco-A, I. Montanari, R. Monkhouse, J. Nelson, J.R. Durrant, J. Phys. Chem. B 105 (31) (2001) 7517–7524.
[12] Masamitsu, H. Miyazaki, K. Matsuhiro, Y. Kumashiro, Y. Takaoka, Solid State Ionics 89 (3,4) (1996) 263–267.
[13] G.R.R.A. Kumaraa, A. Konnoa, G.K.R. Senadeerab, P.V.V. Jayaweerab, D.B.R.A. De Silvab, K. Tennakone, Sol. Energy Mater. Sol. Cells 69 (2) (2001) 195–199.
[14] K. Tennakone, V.P.S. Perera, I.R.M. Kottegoda, G. Kumara, J. Phys. D: Appl. Phys. 32 (4) (1999) 374–379.
[15] T. Kitamura, M. Maitani, M. Matsuda, Y. Wada, S. Yanagida, Chem. Lett. 10 (2001) 1054–1055.
[16] J. Kruger, R. Plass, M. Gratzel, M. Hans-Jorg, Appl. Phys. Lett. 81 (2) (2002) 367–369.
[17] L. Schmidt-Mende, U. Bach, R. Humphry-Baker, T. Horiuchi, H. Miura, S. Ito, S. Uchida, M. Graetzel, Adv. Mater. (Weinheim, Germany) 17 (7) (2005) 813–815.
[18] J. Xia, N. Masaki, M. Lira-Cantu, Y. Kim, K. Jiang, S. Yanagida, J. Am. Chem. Soc. 130 (4) (2008) 1258–1263.
[19] N. Martin, L. Sanchez, B. Illescas, I. Perez, Chem. Rev. 98 (7) (1998) 2527–2547.
[20] S. Saito, A. Oshiyama, Phys. Rev. Lett. 66 (20) (1991) 2637–2640.
[21] A. Skumanich, Chem. Phys. Lett. 182 (5) (1991) 486–490.
[22] M. Hosoya, K. Ichimura, Z.H. Wang, G. Dresselhaus, P.C. Eklund, Phys. Rev. B 49 (7) (1994) 4981–4986.
[23] F. Arias, Q. Xie, Q. Lu, S.R. Wilson, L. Echegoyen, J. Am. Chem. Soc. 116 (1994) 6388–6394.
[24] P.M. Allemand, A. Koch, F. Wudl, Y. Rubin, F. Diederich, M.M. Alvarez, S.J. Anz, R.L. Whetten, J. Am. Chem. Soc. 113 (1991) 1050–1051.
[25] R.S. Flanagan, M.M. Haley, S.O. Brien, C. Pan, Z. Xiao, W.E. Bilups, M.A. Ciufolini, R.H. Hauge, J.L. Margrave, L.J. Wilson, R.F. Curl, R. Smalley, J. Phys. Chem. 94 (1990) 1050–1055.
[26] G. Saito, T. Teramoto, A. Otsuka, Y. Sugita, T. Ban, K. Kusuniki, Synth. Met. 64 (1994) 359–368.
[27] L.S. Wang, J. Conceicao, C. Jin, R. Smalley, Chem. Phys. Lett. 182 (1991) 5–11.
[28] Q. Xie, E. Perez-Cordero, L. Echegoyen, J. Am. Chem. Soc. 114 (1992) 3978–3980.
[29] Y. Ohsawa, T. Saji, J. Chem. Soc. Chem. Commun. (1992) 781–782.
[30] S. Nonell, J.W. Arbogast, C.S. Foote, J. Phys. Chem. 96 (1992) 4169.
[31] C.S. Foote, Top. Curr. Chem. 169 (1994) 347–363.
[32] G. Lem, D.I. Schuster, S.H. Courtney, Q. Lu, S.R. Wilson, J. Am. Chem. Soc. 117 (1995) 554–555.
[33] C. Siedschlag, H. Luftmann, C. Wolff, J. Mattay, Tetrahedron 53 (1997) 3587–3592.
[34] I. Toshiyuki, M. Makoto, M. Kei, H. Shuichi, K.A. Motoi, M. Minoru, Tetrahedron 64 (2008) 1823–1828.
[35] T. Da Ros, M. Prato, F. Novello, M. Maggini, E.J. Banfi, Org. Chem. 61 (1996) 9070–9072.
[36] D.R. Tatiana, P. Maurizio, C. Maurizio, C. Paola, P. Francesco, R. Sergio, J. Am. Chem. Soc. 120 (1998) 11645–11648.
[37] W.S. Shin, H.H. Jeong, M.K. Kim, S.H. Jin, M.R. Kim, J.K. Lee, J.W. Lee, Y.S. Gal, J. Mater. Chem. 16 (2006) 384–390.
[38] S. Seiichi, M. Shogo, S. Sinya, U. Hisanao, S. Eiji, J. Photochem. Photobiol. A: Chem. 194 (2008) 143–147.
[39] K. Tennakone, G.R.R.A. Kumara, A.R. Kumarasinghe, K.G.U. Wijayantha, P.M. Sirimanne, Semicond. Sci. Technol. 10 (12) (1995) 1689–1693.
[40] M. Wang, L. Yang, X. Zhou, Y. Lin, X. Li, S. Feng, X. Xiao, Chin. Sci. Bull. 51 (13) (2006) 1551–1556.
[41] H.M.J.C. Pitawala, M.A.K.L. Dissanayake, V.A. Seneviratne, B.E. Mellander, I. Albinson, J. Solid State Electrochem. 12 (7–8) (2008) 783–789.